Article:
Wang, C, Sivan, M, Wang, D et al. (2022) Quantitative Elbow Spasticity Measurement Based on Muscle Activation Estimation Using Maximal Voluntary Contraction. IEEE Transactions on Instrumentation and Measurement, 71. 4004911. ISSN: 0018-9456

https://doi.org/10.1109/TIM.2022.3173273

Quantitative Elbow Spasticity Measurement Based on Muscle Activation Estimation Using Maximal Voluntary Contraction

Chao Wang, Manoj Sivan, Danyang Wang, Zhi-Qiang Zhang, *Member, IEEE*, Gu-Qiang Li, Tianzhe Bao, and Sheng Quan Xie, *Senior Member, IEEE*

***Abstract*—Conventional measurement of spasticity in stroke patients, e.g., Modified Ashworth Scale (MAS), has been challenged about its reliability issues. Surface Electromyography (sEMG) has been used to identify neuromuscular abnormalities since it directly measures electrical activity in the muscle, however its performance is affected by the placement of electrodes and cross-talk, and it cannot detect the activities of deep muscles. This study proposes a novel spasticity measurement method by quantifying the difference between the impaired and unaffected sides in the elbow maximal voluntary contraction (MVC) task. Five inertial measurement units (IMUs) and a force sensor were used to capture the movement dynamics for the MVC test, by which a neuromusculoskeletal model is established to estimate the muscle activation using the inverse dynamics and optimization techniques. Normalized keeping time of peak activation is a quantitative feature that identifies the disparity between the impaired and unaffected side in the MVC test is defined as a measurement of spasticity. Six stroke patients and eight healthy subjects were recruited to evaluate the muscle activation estimation model. The outcomes of our measurement for patients were compared with the spasticity rated by an experienced physical therapist (PT) using MAS. The estimated muscle activation shows promising accuracy compared to the sEMG profiles (patients: mean $R^2 \approx 0.705$; healthy: mean $R^2 \approx 0.91$). The outcomes of our approach are highly correlated with MAS (Pearson's $r \approx 0.96$, $p < 0.05$). These findings indicate that our approach can provide a quantitative measure of spasticity and can be used as a complementary measurement along with the existing clinical methods. This approach will also enhance the efficiency of upper limb robot-aided rehabilitation in stroke patients.**

***Index Terms*—Biomedical engineering, spasticity measurement, EMG, upper limb, stroke rehabilitation.**

I. INTRODUCTION

Spasticity is a characteristic sensorimotor disorder following stroke. The limitation of joint range of motion and exaggeration of stretch reflexes increase with the severity of spasticity [1], which impacts the life quality for stroke patients and brings challenges to rehabilitation therapies. Previous studies demonstrated that comprehensive evaluation of spasticity improved the efficiency of rehabilitation [2], [3]. Conventionally, the most commonly used spasticity measurement methods in practice are clinical scales, e.g., Modified Ashworth Scale (MAS) [4], [5], and Australian Spasticity Assessment Scale (ASAS) [6]. However, with the clinical scales, the grading depends on assessors' experience so that inexperienced clinicians may not be able to have a precise evaluation [7], [8].

To measure the spasticity more reliably, various approaches were proposed using quantitative measurements [8]–[10], which can be divided into two groups: involuntary-contraction-based and voluntary-contraction-based. Numerous studies utilized the velocity-depended properties of involuntary contraction tasks to assess spasticity [8], [11], [12] based on Lance's definition [13]. Although later studies proposed alternative definitions, Lance's definition remains the most widely accepted one in the literature [14]–[16]. However, stroke patients cannot voluntarily contract the spastic muscles as normal people, which may lead to compensatory movements or even functional impairments. Assessing activities of muscles during voluntary contraction can help improve the understanding of how spasticity affects voluntary contraction.

EMG has been frequently utilized to study the muscle properties, e.g., synergy [17] and spasticity [18], [19], and also muscles' activity. There are two types of EMG detection techniques: Surface Electromyography (sEMG) and intramuscular EMG(iEMG). Although the signal-to-noise ratio (SNR) of iEMG is supposed to be higher than sEMG, its application is restricted due to the invasiveness. By contrast, sEMG is safer and easier to use, and it can be used to detect muscle activities. However, its detection performance is affected by electrodes' placement and cross-talk, thereby it cannot accurately detect the activities of deep muscles [20]. Therefore, a more convenient approach for characterizing muscle activity is desirable. Musculoskeletal models were developed to estimate muscle activation [21], [22]. Raikova et al. presented an elbow musculoskeletal model by which they predicted the muscle forces using the inverse dynamics and optimization techniques based on motion dynamics [23]. Inertial measurement units (IMUs) were utilized for human motion tracking, which is more convenient to use for home-based rehabilitation environment [24], [25].

Wang et al. reported the difference in neuromechanical characteristics for maximum isometrics voluntary contraction

This work is in collaboration with the Institute of Rehabilitation Engineering, Binzhou Medical University, Yantai, 264033, China.(*Corresponding authors: Sheng Quan Xie, Gu Qiang Li.*)

Chao Wang, Zhi Qiang Zhang, and Sheng Quan Xie are with the School of Electrical and Electronic Engineering, University of Leeds, Leeds, LS2 9JT, U.K. (e-mail: elcw@leeds.ac.uk, z.zhang3@leeds.ac.uk, s.q.xie@leeds.ac.uk).

Manoj Sivan is with the Academic Department of Rehabilitation Medicine, University of Leeds, Leeds, LS2 9JT, U.K. (e-mail: m.sivan@leeds.ac.uk).

Danyang Wang and Gu Qiang Li is with the School of Rehabilitation Medicine, Binzhou Medical University, Yantai 264100, China (e-mail: 951656857@qq.com, e-mail: lgq100@bzmc.edu.cn).

Tianzhe Bao is with the Institute of Rehabilitation Engineering, University of Health and Rehabilitation Sciences, Qingdao, China (e-mail: tianzhe.bao@uor.edu.cn).

between the impaired and non-impaired arm of stroke patients [9]. This method cannot quantify the difference across subjects. Ang et al. proposed a neuromusculoskeletal model to quantify the muscle spasticity by estimating the tonic stretch reflex threshold, which only investigated the passive muscle contraction [22]. Nevertheless, understanding how spasticity impacts voluntary contraction is equally important. Moreover, the measurement procedure involved manual operations, which may lead to subjectivity. A recent study was carried out to measure upper-limb spasticity based on the temporal features of reaching movement, which only considered the overall performance of the upper limbs [15]. This method cannot identify spasticity-induced motor deficits of a specific muscle or joint, which means the impact on the motion of a specific muscle cannot be identified.

To overcome the drawbacks of previous spasticity measurement techniques and improve the robustness of muscle activation estimation, we propose a new quantitative spasticity measurement method for the elbow joint on the basis of a neuromusculoskeletal model together with real-time IMU and force sensor measurements. The elbow is modeled as a 1-degree-of-freedom (1-DoF) joint which consists of 5 muscles. A set of IMUs and a force sensor are employed to record the motion and contact force during MVC tests. The muscle activation distribution is estimated with the movement dynamics and the neuromusculoskeletal model. Then, the predicted muscle activation is utilized to calculate the keep time of peak activation, t_k, by which the normalized keep time, $\bar{t_k}$ is figured out to evaluate the severity of spasticity. The main contributions of this study are: 1) a novel measurement of spasticity is developed on the basis of muscle activation estimation; 2) a subject-specific neuromusculoskeletal model is established to estimate the activation of each muscle in the elbow during MVC tests using a set of IMUs and a force sensor; 3) the preliminary validation of this model-based spasticity measurement is presented.

The remaining paper is organized as follows: an overview of the spasticity measurement is described in Section II-A; the neuromusculoskeletal modeling is presented in Section II-B; the spasticity measurement is defined in Section II-C; experiment protocol and data processing is introduced in Section II-D and II-E; validation result and discussion are stated in Section III and IV. Section V summarizes the advantages and limitations, and concludes this paper.

II. METHODOLOGY

A. Overview of Spasticity Measurement

The spasticity measurement method is established on the foundation of muscle activation estimation. Firstly, an elbow musculoskeletal model was created to estimate the joint torque shared by all related muscles. Secondly, a static optimization method was applied to address the muscle-sharing problem so that the muscle force distribution can be determined. Subsequently, the muscle activation is computed by inverting the Hill's muscle-tendon model [31]. Finally, a quantitative measurement method of spasticity is defined as the normalized keeping time of peak activation, see Section II-C for the detailed definition, which is validated in Section III-B. The procedure of the spasticity measurement method is shown in Fig. 1.

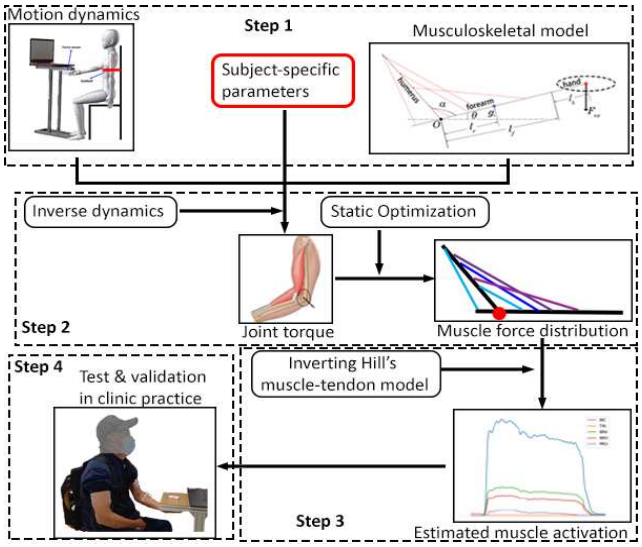

Fig. 1. The four steps of the spasticity measurement based on muscle activation estimation: step 1. collect the subject-specific parameters and movement data; step 2. estimate the muscle force distribution; step 3. compute the muscle activation distribution; step 4. test and validate the spasticity measurement method in clinical practice.

B. Upper-Limb Model

1) Kinematics: Five muscles related to the joint of interest, i.e., the elbow flexion/extension, are considered: biceps brachii (BIC), brachioradialis (BRD), brachialis (BRA), triceps brachii (TRI), and pronator teres (PRO). The joint's range of motion is from 0° to 130°. The determination methods for the subject-specific parameters in this model are summarized in Table.I.

TABLE I
DETERMINATION METHOD OF SUBJECT-SPECIFIC PARAMETERS OF THE MUSCULOSKELETAL MODEL.

Properties	Measurement/Calculation	Note
M_0	Measured Manually	
l_f	Measured Manually	Lateral humeral epicondyle to radial styloid process
M_{fh}	0.022 x M_0	[26]
l_r	0.468 x l_f	[26]

Note. M_0 is the total body mass; l_f is the length of forearm; M_h is the mass of humerus; M_{fh} is the mass of forearm and hand; l_r is the distance between the rotation center of elbow joint and center of mass of forearm and hand.

2) Equation of Motion: Fig. 2 demonstrates the construction of the elbow model, by which the dynamics of this model can be mathematically described as:

$$\tau_g + \tau_{load} + \tau_c + \sum_{i=1}^{m} \tau_i(a_i) = 0 \tag{1}$$

where τ_i is the joint torque produced by the ith muscle; m is the total number of muscles; τ_g is the gravitational term, which can be calculated as:

$$\tau_g = M_{fh} g \times l_r \cos\theta \tag{2}$$

τ_c is the centrifugal term computed as:

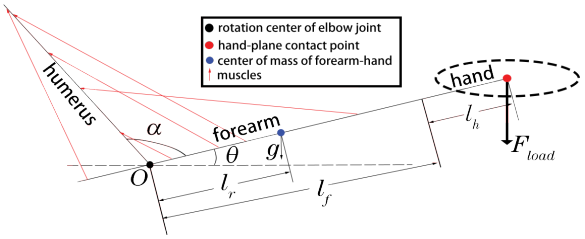

Fig. 2. 1-DoF biomechanical model of elbow joint where l_f is the length of forearm; l_r is the distance from O to the mass center of forearm and hand; g is the gravitational acceleration; α is the joint angle; θ is the angle between the forearm and the horizontal axis; F_{load} is the contact force between hand and the contact plane.

$$\tau_c = I_{fh}\ddot{\alpha}_{fe} \tag{3}$$

where I_{fh} is the moment of inertia of forearm-hand against the elbow joint, $I_{fh} = M_{fh}l_r^2$; α_{fe} is the elbow flexion angle, $\alpha_{fe} = \pi - \alpha$.

The torque contributed by the ith muscle can be calculated as:

$$\tau_i = F_i^{mt} \times MA_i \tag{4}$$

where F_i^{mt} is the muscle-tendon force contributed by ith muscle, which is formulated by the hill-type muscle-tendon model (Detailed information is illustrated in section II-B4). MA_i is the corresponding moment arm against elbow joint which is geometrically related to the muscle fiber length and joint angle, [27]. However, due to the high computational cost, the polynomial equations are used to calculate the moment arms as an alternative in this paper [28].

The joint torque produced by the external force, F_{load} can be written as:

$$\tau_{load} = F_{load} \times (l_f + l_h)\cos\theta \tag{5}$$

3) Optimization: According to section II-B2, the total joint torque contributed by all muscles, $\sum_{i=1}^{m}\tau_i(a_i)$, can be figured out. However, due to the redundancy of UL musculoskeletal system, the solution of muscle force configuration cannot be determined only based on the biomechanical model. In this study, this problem is solved using the optimization technique [29]. The muscle load sharing problem is formulated as:

$$\begin{aligned} &\min J(a_i) = \sum_{i=1}^{5}(\lambda_i F_i^{mt}(a_i))^2 \\ &\text{s.t.} \quad T(a_i) = 0 \end{aligned} \tag{6}$$

where $J(a_i)$ is to minimize the summation of squared muscle stress; λ_i is reciprocal of physiological cross-sectional area (PCSA) of the ith muscle, 1/PCSA$_i$ [30]; $T(a_i)$ is the equation of motion, i.e., Equation (1).

4) Hill's Muscle-tendon Model: Hill-type muscle-tendon model is utilized to formulate the muscle contraction dynamics [31]. The model contains three elements: 1). the contractile element (CE) represents the muscle fibers; 2). the parallel elastic element (PE) represents the passive elastic tissue; 3). the series elastic element (SE) represents the muscle tendon, see Fig.3. The force of CE is formulated as a function of muscle activation, and the force of PE can be calculated based on the optimal fiber length and muscle fiber length. Based on the construction of this model, the muscle-tendon force produced by the ith muscle can be written as:

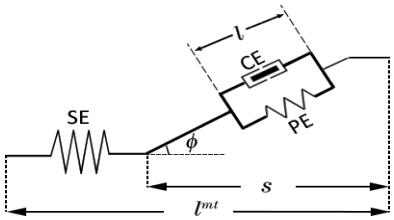

Fig. 3. Hill-type Muscle Tendon Model: ϕ is the angle between muscle fibers and the line action of the muscle, called pennation angle. s is the state variable for the muscle contraction dynamics which can be calculated as: $s = l\cos\phi$.

$$F_i^{mt} = (F_{CE,i} + F_{PE,i})\cos\phi \tag{7}$$

where $F_{CE,i}$ and $F_{PE,i}$ are the force produced by CE and PE of the ith muscle, respectively.

According to the earlier studies, the force produced by CE is determined by the muscle activation level, a, maximal isometric force, F_{max}, muscle fiber length, l_i, and fiber lengthening velocity, $\dot{l}_i$, together. The force produced by CE is obtained as:

$$F_{CE,i} = a_i \cdot F_{max,i} \cdot f_a(\bar{l}_i^a) \cdot g_a(\bar{\dot{l}}_i^a) \tag{8}$$

where $\bar{l}_i^a$ is the normalized muscle fiber length; $\bar{\dot{l}}_i^a$ is the normalized muscle lengthening velocity; $f_a(\cdot)$ and $g_a(\cdot)$ are the force-length-relation and force-velocity-relation for CE, respectively [32], [33].

The passive force generated by PE is calculated as:

$$F_{PE,i} = F_{max,i}\exp(10 * C_{pass}(\bar{l}_i^p - 1))/\exp(5) \tag{9}$$

where C_{pass} is a term accounting the difference across subjects while we set it as 1 for all subjects; $\bar{l}_i^p$ is the normalized muscle fiber length [34], [36]. Consequently, the muscle activation level, a_i, can be estimated by combining Equation (8), (9), and (6).

5) Parameters Tuning: The parameters in the hill's model are tuned manually in this model. The maximal isometric force of muscles, $F_{max,i}$, and the optimal fiber lengths of all muscles are scaled from a generic model [37]. The scale factors are calculated based on the manual measurement of related segments. While, $F_{max,i}$ is tuned empirically to minimize error between the estimated biceps brachii activation and the sEMG-based muscle activation, see Equation (11). Additionally, the pennation angle of each muscle (angle between muscle fiber and the line of action) is assumed as 0 (The pennation angles are constant during the contraction so that the $\cos\phi$ are constant as well. Thus, the impact is linear and can be countered by tuning other parameters like $F_{max,i}$ when we set ϕ as 0).

C. Spasticity Quantification

Based on Section II-B3, the muscle activation of MVC test can be estimated:

$$A_n = \arg\min_{T(a_{i,n})=0} J(a_{i,n}) \tag{10}$$

where A_n is$\{a_1, a_2, a_3, a_4, a_5\}$, n is the frame number which is from 1 to N (N is the total frame number of one test). Then, the peak activation is defined as: $a_{i,peak} = \max\{a_{i,n}\}$. The keeping time of peak activation of the spastic arm was found to be shorter than the healthy arm [9]. This is probably because the exaggeration of stretch reflexes increases with the severity of spasticity so that the affected muscles would tire quicker than non-affected muscles. The method we proposed is modified to match the UL model in Section II-B whose output is muscle activation. As shown in Fig. 4, the peak activation of one muscle is used to define the muscle strength represented by a_{peak}. The time length of keeping the peak activation (above the 40% of peak activation, $0.4a_{peak}$), t_k is extracted to account for the patients' ability to contain the spasticity.

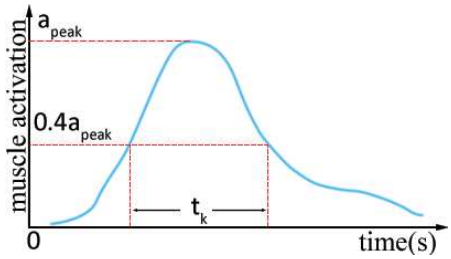

Fig. 4. Description of the features extracted from the predicted muscle force.

However, due to the difference across subjects, t_k can not be used to assess the severity of spasticity directly. In this study, t_k of patients' affected side is normalized to their healthy side, which is obtained as: $\bar{t_k} = t_{k,a}/t_{k,h}$, where $t_{k,a}$ is the t_k for affected side, $t_{k,h}$ is the t_k for healthy side. In the rest of this paper, we will use $\bar{t}_{k,1}$, and $\bar{t}_{k,2}$ to represents the feature, t_k of biceps brachii and brachialis, respectively.

D. Experimental Setup

1) Testing Protocol: The demographics of the participants are documented, including the name, age, gender, affected side (patients only), time from stroke onset (patients only), and the severity of spasticity (patients only) of the elbow joint is evaluated by an experienced Physical Therapist(PT) using MAS. The five IMUs and a sEMG sensor are attached to the subject as shown in Fig.5(a).

The MVC test has four tasks to be completed for each side of the subject. The data from the first task is used to tune the parameters in the neuromusculoskeletal model, and the rest of the data is used for the validation of the spasticity measurement method. In each task, the subjects are required to do the MVC task by holding and pressing the contact plate of the force measurement device for as long as possible, see Fig. 5(b). After each task, the subjects have 5 minutes break to allow the muscle force and endurance to recover [38]. The contact force is measured at 90 Hz by a force sensor. The muscle activity of the biceps brachii is recorded by an sEMG sensor at 2000 Hz, and kinematic data of the tested side is captured by 5 IMUs at 200 Hz. Both sides of the arm are repeated for all the subjects. This study has been reviewed and approved by the Ethics Committee of the Yantai Affiliated Hospital of Binzhou Medical University.

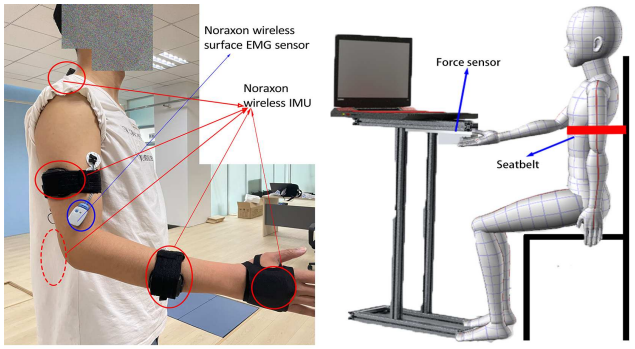

Fig. 5. (a) The placement of IMUs and sEMG sensors: three IMUs for the arm of each side, and two IMUs are placed at 7^{th} cervical vertebra (C7) and 10^{th} thoracic vertebra (T10), respectively. The sEMG sensor is attached on biceps brachii. (b) Experimental setup for spasticity measurement: subject sits in front of the force measurement device with a seatbelt fastened to avoid compensatory movements. A force sensor is installed on the side of the table plate facing the ground, and it is synchronized with the IMUs and sEMG sensor through a trigger signal generator.

TABLE II
INFORMATION OF THE STROKE PATIENTS

Sub ID	Gender	Age	H (cm)	W (kg)	Affected side	t_{on}
S1	M	45	173	87.8	R	$\geq$12
S2	M	66	160	75.5	R	$\geq$12
S3	F	53	158	60.5	L	$\geq$12
S4	M	44	162	68.5	L	$\geq$12
S5	M	48	167	81.0	R	$\geq$12
S6	M	55	175	90.0	L	$\geq$12

Note. H is the height; W is the weight; t_{on} is the time since stroke onset (month).

2) Participant Information: Six post-stroke patients were enrolled in this study, aged 44-66 years. The admission criteria of stroke participants were: (1) at least six months from onset of stroke; (2) being able to complete the experimental tasks independently; (3) elbow spasticity score(MAS) of the affected side is 0, or 1, 1+ or 2(patients with severer spasticity generally cannot contract the related muscles voluntarily); (4) being able to read the study information and give informed consent; (5) right-dominant. The patients with the following conditions were excluded: (1) cognitive dysfunction, (2) both sides are affected. Additionally, eight healthy subjects are recruited to investigate the healthy patterns and verify the muscle activation estimation model's performance. The summarized information of the patients and healthy participants are listed in Table.II and Table. III, respectively.

E. Data Preprocessing

1) Surface EMG: The muscle activation interpreted from sEMG data is compared with the predicted muscle activation. Firstly, the raw sEMG signals are rectified [34] after being filtered by a 4^{th} order bandpass filter from 20 to 500 Hz. Then, a moving average filter is applied with the time window T_w=88 ms, and the filtered signals are low-pass filtered by a 2^{rd} order Butterworth filtered at 2 Hz. Subsequently, the signals are normalized to the peak value, and the resultant muscle activation level can be formulated by the following equation:

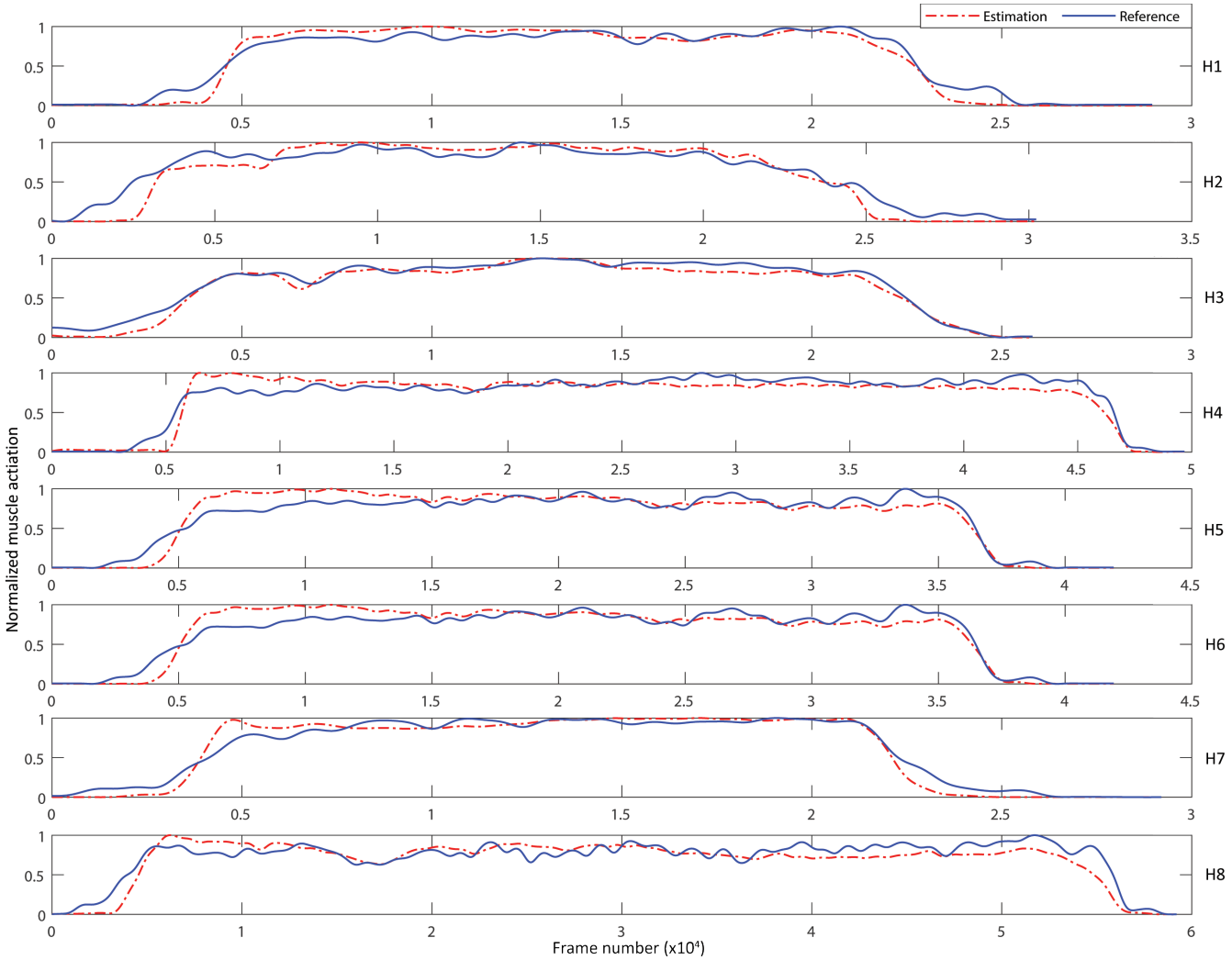

Fig. 6. Comparison of the muscle activation predicted by the model and interpreted from sEMG signals of biceps brachii of 8 healthy subjects. Blue line: muscle activation interpreted from sEMG data; red line: muscle activation predicted by the model. The cross-correlations between the two lines of subject H1 to H8 are: 0.98, 0.96, 0.98, 0.94, 0.96, 0.95, 0.98, and 0.91, respectively.

TABLE III
INFORMATION OF THE HEALTHY PARTICIPANTS

Sub ID	Gender	Age	H (cm)	W (kg)
H1	M	22	187.5	102.0
H2	M	23	175.0	76.5
H3	M	22	186.0	74.5
H4	M	24	181.0	71.0
H5	F	24	158.0	45.0
H6	F	25	169.5	66.0
H7	F	26	164.0	60.5
H8	M	23	158.0	66.5

Note. All healthy participants are right-dominant.

$$a_i(t) = \frac{e^{AU_i(t)} - 1}{e^A - 1} \tag{11}$$

where $U_i(t)$ is the processed sEMG signals for i^{th} muscle, A is the corresponding nonlinear shape factor which is allowed to vary between -3 and 0 [33]–[35]. In this study, A is tuned empirically to minimize the errors between the muscle activation extracted from biceps brachii sEMG signals and the model's output (only the data of the first motor task is used to tune A, and other parameters, which will not be used for the validation of muscle activation estimation and spasticity measurement).

2) Contact Force & IMU: To apply the force signals and IMU signals together with the model, the raw force signals are interpolated to match the length of sEMG signals using B-spline algorithm. Then, a 2nd order low-pass Butterworth filter is applied with the corner frequency at 10 Hz. The motion data captured by IMUs is processed to extract the joint motion.

III. RESULTS

A. Validation of Muscle Activation Estimation Model

As the muscle forces are not measurable, there is no standard and direct way to validate the muscle force/activation estimated by the models. According to the literature [21], [22], we evaluate the prediction result by comparing the model's output against the sEMG data. The comparison result (cross-correlation) of 8 healthy individuals and 6 patients is shown in Fig. 6, and Fig. 7, respectively. In addition, the root-mean-squared-error ($RMSE$) and coefficient of determination (R^2) between them are calculated to evaluate the amplitude error

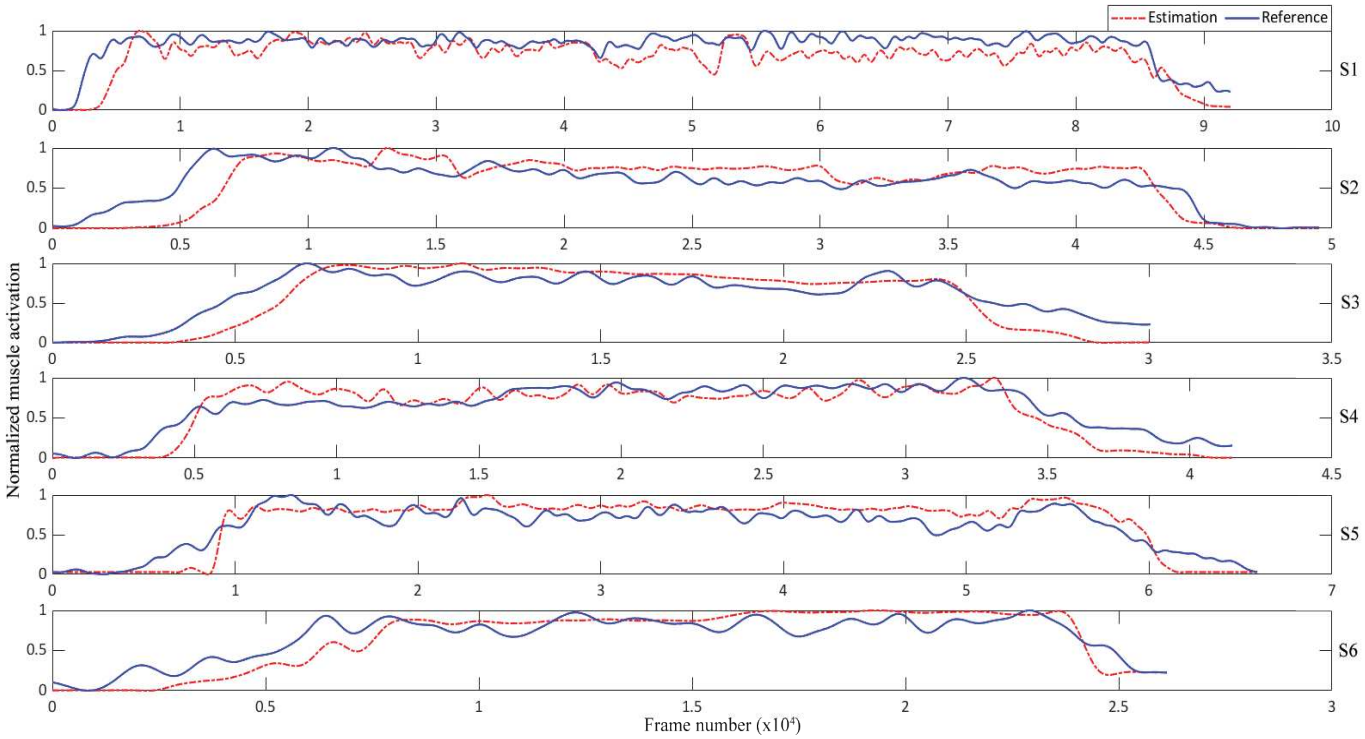

Fig. 7. Comparison of the muscle activation predicted by the model and interpreted from sEMG signals of biceps brachii of 6 patients. Blue line: muscle activation interpreted from sEMG data; red line: muscle activation predicted by the model. The cross-correlations between the two lines of subject S1 to S6 are: 0.82, 0.81, 0.91, 0.92, 0.92, and 0.91, respectively.

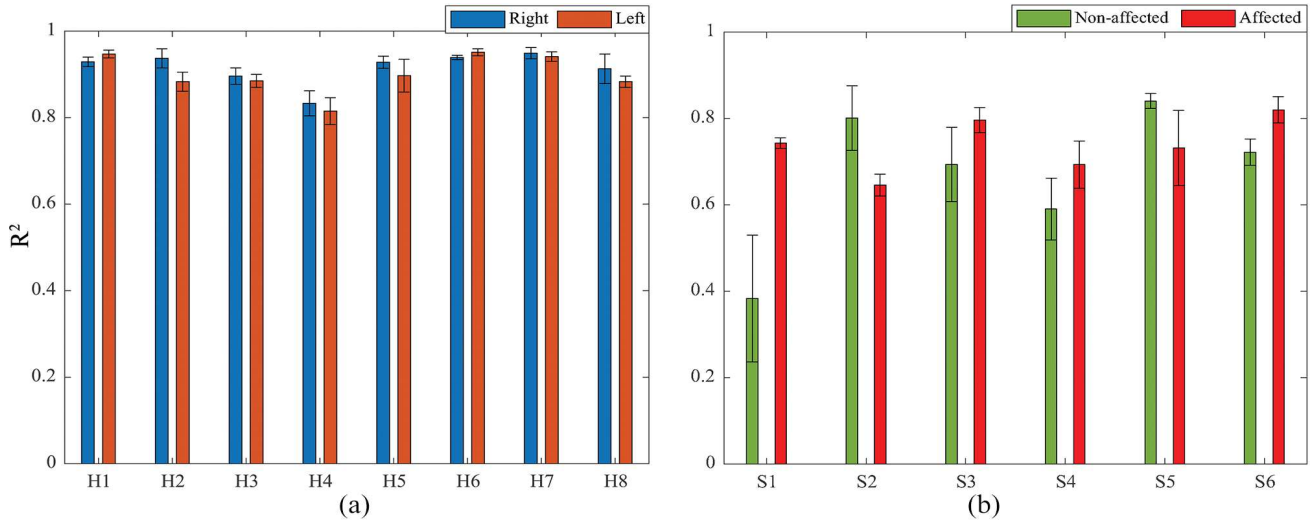

Fig. 8. (a) Mean R^2 of both sides of the healthy individuals; (b)Mean R^2 of both sides of the patients.

and goodness of fit. $RMSE$ and R^2 are obtained by the following equations:

$$RMSE = \sqrt{\frac{1}{N}\sum_{i=1}^{N}(a_i - \widehat{a}_i)^2} \tag{12}$$

$$R^2 = 1 - \frac{\sum_{i=1}^{N}(a_i - \widehat{a}_i)^2}{\sum_{i=1}^{N}(a_i - \overline{a}_i)^2} \tag{13}$$

where N is the total frame number, a_i is the muscle activation of ith muscle interpreted from sEMG, $\widehat{a}_i$ is the corresponding estimated muscle activation, $\overline{a}_i$ is the mean of a_i.

The R^2 validation result of patient and healthy participants are shown in Fig.8(a) and Fig. 8(b), respectively. Table. IV and V shows the $RMSE$ between the muscle activation interpreted from sEMG and the model's estimation. For most patients, the mean R^2 is higher than 0.6 with $RMSE$ lower than 0.25. In the healthy participants, the mean $RMSE$ of every subject is lower than 0.15; and the mean R^2 is higher than 0.87.

Although the estimated muscle activation shows a good correlation with sEMG in the healthy participants, we still need to verify if the estimation and sEMG are consistent in $\bar{t_k}$. $\bar{t_k}$ is computed from predicted muscle activation to compare with that extracted from the sEMG data.

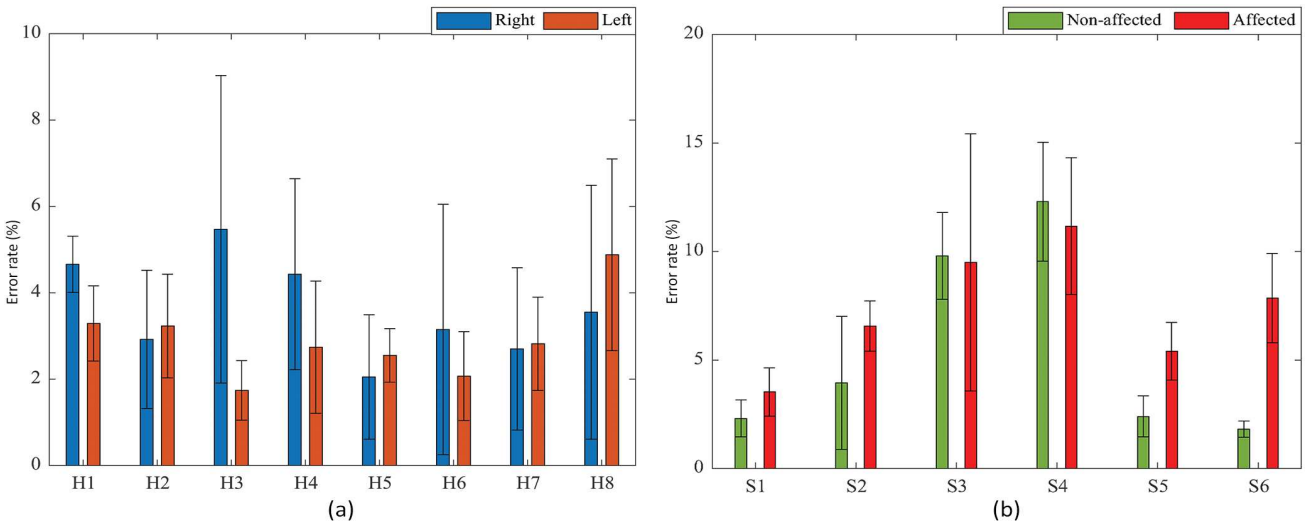

Fig. 9. (a) Mean error rate between sEMG-based $\bar{t_k}$ and estimation-based $\bar{t_k}$ for both sides of the healthy individuals. (b) Mean error rate between sEMG-based $\bar{t_k}$ and estimation-based $\bar{t_k}$ for both sides of the patients.

TABLE IV
$RMSE$ BETWEEN THE MUSCLE ACTIVATION INTERPRETED FROM SEMG SIGNALS AND ESTIMATED BY THE MODEL FOR PATIENTS

	Non-affected		Affected	
ID	Mean $RMSE$	$std.$	Mean $RMSE$	$std.$
S1	0.1711	0.0298	0.1399	0.0091
S2	0.1385	0.0176	0.1992	0.0152
S3	0.1842	0.0105	0.1443	0.0293
S4	0.2473	0.0264	0.1949	0.0208
S5	0.0978	0.0098	0.1607	0.0156
S6	0.1538	0.0069	0.1032	0.0151

$std.$ = standard deviation

TABLE V
$RMSE$ BETWEEN THE MUSCLE ACTIVATION INTERPRETED FROM SEMG SIGNALS AND THE MODEL'S ESTIMATION FOR HEALTHY PARTICIPANTS

	Right		Left	
ID	Mean $RMSE$	$std.$	Mean $RMSE$	$std.$
H1	0.103	0.006	0.089	0.002
H2	0.093	0.018	0.114	0.005
H3	0.114	0.019	0.107	0.001
H4	0.141	0.006	0.122	0.011
H5	0.116	0.012	0.119	0.016
H6	0.105	0.005	0.096	0.007
H7	0.089	0.007	0.094	0.008
H8	0.107	0.011	0.127	0.021

In the healthy participants, the error rate of the estimation-based $\bar{t_k}$ is calculated and shown in Fig. 9(a). The mean error rate of every single subject is lower than 6%. In the patient group, the comparison result is summarized in Fig. 9(b). The mean error rate of $\bar{t_k}$ is lower than 14% for every subject. The error rate of $\bar{t_k}$ is defined as:

$$ER = \frac{|\bar{t}_{k,sEMG} - \bar{t}_{k,estimation}|}{\bar{t}_{k,sEMG}} \quad (14)$$

The Analysis of Variance (ANOVA) test was used to validate the difference in the muscle activation estimation model's performance between the two sides of healthy individuals and the two sides of patients. The difference between healthy individuals and patients was also validated. The three hypotheses were: H_0: the difference between the two sides of healthy individuals is not significant; H_1: the difference between the two sides of patients is not significant; H_2: the difference between patients and healthy individuals is not significant. Table VI shows the result of ANOVA test, which indicates that the muscle activation estimation model's performance is at the same accuracy level for healthy individuals and the patients' two sides, while the difference between healthy individuals and patients is significant.

TABLE VI
THE ANOVA-TEST RESULT OF THE HYPOTHESIS, H_0, H_1 AND H_2

Pair	f	p	Result
H two sides	0.538	0.475	Accept H_0
S two sides	0.838	0.382	Accept H_1
H and S	37.044	1.97×10^{-6}	Reject H_2

H: healthy individuals; S: stroke patients.

Additionally, the difference in the error rates of the estimated $\bar{t_k}$ between the two sides of healthy individuals, the two sides of patients, and the two groups are validated based on ANOVA test. Three more hypotheses are made: $H_{0,tk}$: the difference of the error rates of the $\bar{t_k}$ between the two sides of healthy individuals is not significant; $H_{0,tk}$: the difference of the error rates of the $\bar{t_k}$ between the two sides of healthy individuals is not significant; $H_{1,tk}$: the difference of the error rates of the $\bar{t_k}$ between the two sides of the patients is not significant; $H_{2,tk}$: the difference of the error rates of the $\bar{t_k}$ between the two groups is not significant. The result illustrates that the error rates of estimated $\bar{t_k}$ between healthy individuals' two sides are at the same level, as well as the patients. However, the difference in error rates between the two groups is significant.

TABLE VII
THE ANOVA-TEST RESULT OF THE HYPOTHESIS, H_0, H_1 AND H_2

Pair	f	p	Result
H two sides	1.770	0.205	Accept $H_{0,tk}$
S two sides	0.787	0.396	Accept $H_{1,tk}$
H and S	10.362	0.003	Reject $H_{2,tk}$

B. Validation of Spasticity Measurement Using the Estimated Muscle Activation during MVC

The most commonly used spasticity measurement method in clinical practice is MAS. As a result, it is adapted as a benchmark by the recent studies [9], [22]. In this study, MAS is utilized to verify the proposed spasticity measurement method in Section II-C. With the muscle activation prediction model, the neuromechanical feature, $\bar{t}_{k,1}$ and $\bar{t}_{k,2}$, is calculated based on the estimated muscle activation of the biceps brachii and brachialis, respectively. Table VIII summarizes the subject's MAS score, $\bar{t}_{k,1}$ and $\bar{t}_{k,2}$, and their corresponding rank among all subjects. The rank is determined by how the $\bar{t}_k$ is closer to 1, and the closest one is ranked as 1. Among the healthy subjects, $\bar{t_k}$ is very close to 1, see Table IX. The result illustrates that the ranks of both are well correlated to MAS scores, both with Pearson's $r \approx 0.96$ ($p < 0.05$).

TABLE VIII
$\bar{t}_{k,1}$ AND $\bar{t}_{k,2}$ CALCULATED BASED ON THE ESTIMATED MUSCLE ACTIVATION AND MAS SCORES OF PATIENTS. THE RANK OF $\bar{t}_{k,1}$ AND $\bar{t}_{k,2}$ ARE DETERMINED BY THE ABSOLUTE VALUE OF THEIR DIFFERENCE TO 1, THE SMALLEST DIFFERENCE IS RANKED AS 1. MAS IS RANKED ACCORDING TO THE SCORE ($0 > 1 > 1+$).

Sub ID	$\bar{t}_{k,1}$	Rank	$\bar{t}_{k,2}$	Rank	MAS	Rank
S1	0.5317	5	0.5335	5	1+	4
S2	0.8796	2	0.8833	2	0	1
S3	1.0111	1	1.0075	1	0	1
S4	0.8378	3	0.8564	3	1	3
S5	0.6137	4	0.6421	4	1+	4
S6	0.2367	6	0.2358	6	2	6

TABLE IX
$\bar{t}_{k,1}$ CALCULATED BASED ON THE EMG DATA OF THE HEALTHY SUBJECTS.

Sub ID	$\bar{t}_{k,1}$
H1	0.9620
H2	1.1270
H3	1.0834
H4	0.9494
H5	0.9757
H6	1.0012
H7	0.8525
H8	0.9023

TABLE X
THE T-TEST RESULT OF THE HYPOTHESIS, H_3 WITH SIGNIFICANCE LEVEL α AT 0.05, CRITICAL VALUE $t_{critical}$ = 2.353, AND NUMBER OF SAMPLE n = 5.

Pair	n	r	α	$t_{critical}$	t	Result
$\bar{t}_{k,1}$ and MAS	5	0.96	0.05	2.132	7.251	Reject H_3
$\bar{t}_{k,2}$ and MAS	5	0.96	0.05	2.132	7.251	Reject H_4

The correlation is tested via t-test. There are two null hypotheses: H_3, there is no correlation between the severity rankings between $t_{k,1}^{-}$ and MAS; H_4, there is no correlation between the severity rankings between $t_{k,2}^{-}$ and MAS. The result is shown in Table. X. Both H_3 and H_4 are rejected, which indicates that the outcome of the model-based spasticity measurement method is highly correlated with MAS.

IV. DISCUSSION

Spasticity is commonly measured based on passive contraction. However, identifying the impact of spasticity on voluntary contraction is also important for planning the rehabilitation training and needs to be further studied. Many recent studies try to evaluate the spasticity using sEMG, while the outcome of sEMG is significantly affected by the placement of electrodes and cross-talk. Moreover, sEMG cannot detect the activity of deep muscles. To this end, we propose the spasticity measurement method based on the muscle activation estimation of MVC to investigate the impacts of spasticity on voluntary contraction. Although the recruited subjects of the two groups are distributed at different age ranges, it will not cause derogatory effect on the spasticity measurement since the model is subject-specific and both the estimation of muscle activation and $\bar{t_k}$ for each subject are independent from others. The performance of the muscle activation prediction model and the model-based spasticity measurement method is discussed in the following two sections.

A. Muscle Activation Estimation

The error between estimation and reference muscle activation is relatively high at the initial and final phases of the MVC test, see Fig. 6. The reason might be that the model does not include the translational movements of both phases. However, the related muscles are activated to drive UL during the UL translation. Consequently, sEMG shows that the muscles are activated at this stage while the estimation result does not. Nevertheless, the estimated muscle activation and sEMG profiles are on the same trend in general, especially in the middle phase, during which they are highly correlated with promisingly low errors, see Fig. 6. Correspondingly, the mean R^2 of both sides of all healthy participants is encouragingly high(lowest mean $R^2 \geq 0.80$), see Fig. 8(a), and the mean $RMSE$ is relatively low (highest mean $RMSE \leq 0.15$), see Table. V, which illustrates the model can well predict the muscle activation during the MVC test for both sides of healthy participants. In the patient group, the result demonstrates a relatively accurate estimation of muscle activation, and the mean R^2 is higher than 0.6 with mean $RMSE$ being lower than 0.25 for most of the patients. Moreover, the standard deviations of both R^2 and $RMSE$ are low, which indicates that the model can predict muscle activation reliably. However, both R^2 and $RMSE$ of healthy participants are better than patients, and the standard deviations of R^2 and $RMSE$ are lower for healthy participants than patients. These are confirmed by the ANOVA tests, see Table. VI. Similarly, in the estimation of $\bar{t_k}$, both the error rate between healthy individuals' and the patients' two sides do not have a significant difference, while the difference between the two groups is significant, see Table VII. The reason might be: 1. the patients cannot complete the MVC tasks as stable as healthy subjects, thereby the displacement of uninvolved UL segments influences the estimation result of patients more than healthy participants; 2. The experiments of patients were taken in the clinical environment where more magnetic noise was detected, which may affect the IMUs detection. Additionally, R^2 of the

non-affected side of subject S1 is much lower than any other subject, and the standard deviation of R^2 is relatively high, see Fig. 8(b). The reason might be that S1 performed more UL displacements than other subjects (the recorded motion data confirmed this conjecture).

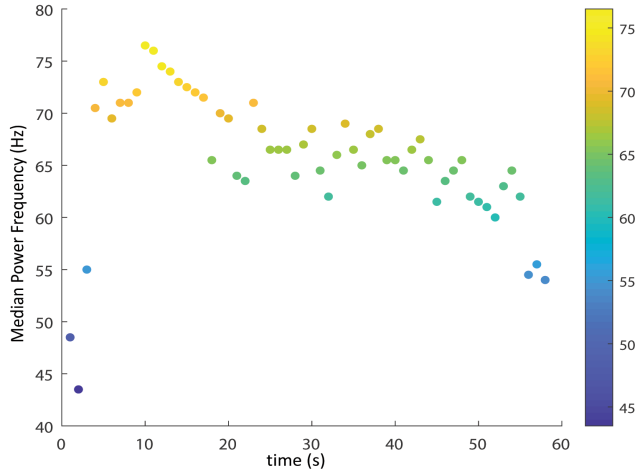

Fig. 10. The median power frequency of the sEMG data changes through time.

The error between estimation and reference is relatively higher in the early stages of the middle phase of the MVC test than in other stages. The reason might be that the muscle fatigue decreases the $F_{max,i}$ [39]. However, as mentioned in section II-B4, $F_{max,i}$ of all muscles are considered as constant, while the value of $F_{max,i}$ will decrease if the muscle fatigue happens. More specifically, the activation level required to produce the same joint torque would change with the changes in muscle fatigue conditions. Thus, the correlation between the prediction and reference muscle activation changes with different stages of the MVC test. The power spectrum is computed to investigate muscle conditions during the MVC test. The result illustrates that the median power frequency (MPF) [40] decreases with the increase of time after reaching the maximal MPF at the beginning of the test, which illustrates the change in muscle fatigue condition, see Fig. 10.

The t_k computed from the muscle activation prediction shows promising high accuracy compared with that from the sEMG data. The mean error rate of t_k for the healthy subject is lower than 6%. In the patient group, this number is lower than 14%. The results suggest that the predicted muscle activation can be used to determine t_k. However, Fig. 9(a) and Fig. 9(b) show that std of the error rate of the t_k obtained from the prediction result is relatively higher for some of the subjects. The reason might be that the estimation results are affected by the movements of unconsidered UL segments at the initial stage of the test. Therefore, the muscle activation in the estimation profile is close to zero in the initial stage when the related muscles are actually activated, which can be seen in the sEMG profile. It means the mean error rate of t_k for the subject heavily depends on the time length of the initial stage. Thus, the error rate would be high if the subject moves too slow initially; conversely, the error rate would be low if the subject moves faster (but does not impact the estimation result of the middle phase).

B. Correlation Between Model's Outcome and Clinical Scale

The model-based outcomes show a high correlation ($r \approx 0.95$, with $p < 0.05$) with MAS scores rated by the PT. This indicates that: 1. The estimated muscle activation is relatively accurate for predicting $\bar{t}_k$; 2. $\bar{t}_k$ can be a potential benchmark for measuring the severity of spasticity. However, only patients rated as 0, 1, 1+ and 2 (MAS) are involved as it would be too hard for patients rated as 3 or above to complete the assessment tasks. Thus, this model-based spasticity measurement method can be used to identify the muscle's state of voluntary contraction. Especially in the home-based environment, this method is easier and more affordable than other spasticity measurement techniques that require clinical knowledge and expensive devices.

V. CONCLUSIONS AND FUTURE WORK

In this paper, we presented a novel quantitative spasticity measurement method, including a neuromusculoskeletal model and a spasticity assessment technique based on muscle activation estimation. The experimental results showed that the estimation of muscle activation is highly correlated with the sEMG profiles (with mean $R^2 \approx 0.705$ for the patient group and 0.91 for the healthy participant group). The results also showed that the outcome of our method is well correlated with the MAS scores given by the PT(with Pearson's $r \approx 0.96$, $p < 0.05$). This indicated the proposed model-based quantitative spasticity measurement method provides accurate clinical assessment for stroke patients. This method does not require a clinic setting for users, which will potentially benefit home-based rehabilitation. There are two main limitations to the proposed method. Firstly, the translational movement is not accounted for in the dynamic model. Secondly, muscle fatigue and muscle co-activation factors are not considered in the muscle dynamics. They will affect the muscle activation estimation and reduce the accuracy of the spasticity measurement. The proposed method will be computationally expensive in order to tune the parameters of the neuromusculoskeletal model. To address this issue, our future work will include new tuning techniques with less computational cost, investigation of the complexity of the model and its relation to the computational cost, and a sensitivity study on the parameters of the proposed model. Further studies will also need to be carried out to improve the accuracy of the muscle activation estimation model.

REFERENCES

[1] B. B Bhakta, "Management of spasticity in stroke," *Br. Med. Bull.*, vol. 56, no. 2, pp. 476-485, 2000.
[2] T. Watanabe, "Assessment of Spasticity in the Upper Extremity," *Spasticity*, 2015.
[3] Y. Yang, Z. Emzain and S. Huang, "Biomechanical Evaluation of Dynamic Splint Based on Pulley Rotation Design for Management of Hand Spasticity," *IEEE Trans. Neural Syst. Rehabil. Eng.*, vol. 29, pp. 683-689, 2021.
[4] Ashworth B, "Preliminary trial of carisoprodol in multiple sclerosis," *Practitioner*, pp. 540-542, 1964.
[5] R. Bohannon and M. Smith, "Interrater Reliability of a Modified Ashworth Scale of Muscle Spasticity," *Phys. Ther.*, vol. 67, no. 2, pp. 206-207, 1987.

[6] S. Love, N. Gibson, N. Smith, N. Bear and E. Blair, "Interobserver reliability of the Australian Spasticity Assessment Scale (ASAS)," *Dev. Med. Child Neurol.*, vol. 58, pp. 18-24, 2016.

[7] M. Blackburn, P. van Vliet and S. Mockett, "Reliability of Measurements Obtained With the Modified Ashworth Scale in the Lower Extremities of People With Stroke," *Phys. Ther.*, vol. 82, no. 1, pp. 25-34, 2002.

[8] S. Dehem et al., "Assessment of upper limb spasticity in stroke patients using the robotic device REAplan," *J. Rehabil. Med.*, vol. 49, no. 7, pp. 565-571, 2017.

[9] H. Wang, P. Huang, X. Li, O. Samuel, Y. Xiang and G. Li, "Spasticity Assessment Based on the Maximum Isometrics Voluntary Contraction of Upper Limb Muscles in Post-stroke Hemiplegia," *Front. Neurol.*, vol. 10, 2019.

[10] S. Li, J. Liu, M. Bhadane, P. Zhou and W. Rymer, "Activation deficit correlates with weakness in chronic stroke: Evidence from evoked and voluntary EMG recordings," *Clin. Neurophysiol.*, vol. 125, no. 12, pp. 2413-2417, 2014.

[11] B. Hu et al., "Spasticity Measurement Based on the HHT Marginal Spectrum Entropy of sEMG Using a Portable System: A Preliminary Study," *IEEE Trans. Neural Syst. Rehabil. Eng.*, vol. 26, no. 7, pp. 1424-1434, 2018.

[12] C. McGibbon, A. Sexton, M. Jones and C. O'Connell, "Elbow spasticity during passive stretch-reflex: clinical evaluation using a wearable sensor system," *J. NeuroEng. Rehabil.*, vol. 10, no. 1, p. 61, 2013.

[13] J. Lance, "The control of muscle tone, reflexes, and movement: Robert Wartenbeg Lecture," *Neurology*, vol. 30, no. 12, pp. 1303-1303, 1980.

[14] S. Li, "Spasticity, Motor Recovery, and Neural Plasticity after Stroke," *Front. Neurol.*, vol. 8, 2017.

[15] G. Mochizuki, A. Centen, M. Resnick, C. Lowrey, S. Dukelow and S. Scott, "Movement kinematics and proprioception in post-stroke spasticity: assessment using the Kinarm robotic exoskeleton," *J. NeuroEng. Rehabil.*, vol. 16, no. 1, 2019.

[16] N. Finnerup, "Neuropathic pain and spasticity: intricate consequences of spinal cord injury," *Spinal Cord*, vol. 55, no. 12, pp. 1046-1050, 2017.

[17] Y. Sheng, J. Zeng, J. Liu and H. Liu, "Metric-based Muscle Synergy Consistency for Upper Limb Motor Functions," *IEEE Trans. Instrum. Meas.*, pp. 1-1, 2021.

[18] X. Zhang, X. Tang, X. Zhu, X. Gao, X. Chen and X. Chen, "A Regression-Based Framework for Quantitative Assessment of Muscle Spasticity Using Combined EMG and Inertial Data From Wearable Sensors," *Front. Neurosci.*, vol. 13, 2019.

[19] T. Xie et al., "Increased Muscle Activity Accompanying With Decreased Complexity as Spasticity Appears: High-Density EMG-Based Case Studies on Stroke Patients," *Front. Bioeng. Biotechnol.*, vol. 8, 2020.

[20] T. Bao, S. Zaidi, S. Xie, P. Yang and Z. Zhang, "A CNN-LSTM Hybrid Model for Wrist Kinematics Estimation Using Surface Electromyography," *IEEE Trans. Instrum. Meas.*, vol. 70, pp. 1-9, 2021.

[21] A. Erdemir, S. McLean, W. Herzog and A. van den Bogert, "Model-based estimation of muscle forces exerted during movements," *Clin. Biomech.*, vol. 22, no. 2, pp. 131-154, 2007.

[22] W. Ang, H. Geyer, I. Chen and W. Ang, "Objective Assessment of Spasticity With a Method Based on a Human Upper Limb Model," *IEEE Trans. Neural Syst. Rehabil. Eng.*, vol. 26, no. 7, pp. 1414-1423, 2018.

[23] R. Raikova, D. Gabriel and H. Aladjov, "Experimental and modelling investigation of learning a fast elbow flexion in the horizontal plane," *J. Biomech.*, vol. 38, no. 10, pp. 2070-2077, 2005.

[24] A. Karime, M. Eid, H. Dong, M. Halimi, W. Gueaieb and A. El Saddik, "CAHR: A Contextually Adaptive Home-Based Rehabilitation Framework," *IEEE Trans. Instrum. Meas.*, vol. 64, no. 2, pp. 427-438, 2015.

[25] J. Li et al., "Using Body Sensor Network to Measure the Effect of Rehabilitation Therapy on Improvement of Lower Limb Motor Function in Children With Spastic Diplegia," *IEEE Trans. Instrum. Meas.*, vol. 69, no. 11, pp. 9215-9227, 2020.

[26] D. A. Winter, *Biomechanics and motor control of human movement*. Hoboken, NJ, USA: Wiley, 2009.

[27] S. Delp et al., "OpenSim: Open-Source Software to Create and Analyze Dynamic Simulations of Movement," *IEEE Trans. Biomed. Eng.*, vol. 54, no. 11, pp. 1940-1950, 2007.

[28] J. Ramsay, B. Hunter and R. Gonzalez, "Muscle moment arm and normalized moment contributions as reference data for musculoskeletal elbow and wrist joint models," *J. Biomech.*, vol. 42, no. 4, pp. 463-473, 2009.

[29] R. Raikova and H. Aladjov, "The Influence of the Way the Muscle Force is Modeled on the Predicted Results Obtained by Solving Indeterminate Problems for a Fast Elbow Flexion," *Comput. Methods Biomech. Biomed. Eng.*, vol. 6, no. 3, pp. 181-196, 2003.

[30] M. Martin, K. Travouillon, P. Fleming and N. Warburton, "Review of the methods used for calculating physiological cross-sectional area (PCSA) for ecological questions," *J. Morphol.*, vol. 281, no. 7, pp. 778-789, 2020.

[31] A. Hill, "The heat of shortening and the dynamic constants of muscle," *Proc. R. Soc. London, Ser. B*, vol. 126, no. 843, pp. 136-195, 1938.

[32] D. Thelen, "Adjustment of Muscle Mechanics Model Parameters to Simulate Dynamic Contractions in Older Adults," *J. Biomech. Eng.*, vol. 125, no. 1, pp. 70-77, 2003.

[33] D. Lloyd and T. Besier, "An EMG-driven musculoskeletal model to estimate muscle forces and knee joint moments in vivo," *J. Biomech.*, vol. 36, no. 6, pp. 765-776, 2003.

[34] T. Buchanan, D. Lloyd, K. Manal and T. Besier, "Neuromusculoskeletal Modeling: Estimation of Muscle Forces and Joint Moments and Movements from Measurements of Neural Command," *J. Appl. Biomech.*, vol. 20, no. 4, pp. 367-395, 2004.

[35] Y. Zhao, Z. Zhang, Z. Li, Z. Yang, A. Dehghani-Sanij and S. Xie, "An EMG-Driven Musculoskeletal Model for Estimating Continuous Wrist Motion," *IEEE Trans. Neural Syst. Rehabil. Eng.*, vol. 28, no. 12, pp. 3113-3120, 2020.

[36] J. Pau, S. Xie and A. Pullan, "Neuromuscular Interfacing: Establishing an EMG-Driven Model for the Human Elbow Joint," *IEEE Trans. Biomed. Eng.*, vol. 59, no. 9, pp. 2586-2593, 2012.

[37] K. Holzbaur, W. Murray and S. Delp, "A Model of the Upper Extremity for Simulating Musculoskeletal Surgery and Analyzing Neuromuscular Control," *Ann. Biomed. Eng.*, vol. 33, no. 6, pp. 829-840, 2005.

[38] K. Sahlin and J. Ren, "Relationship of contraction capacity to metabolic changes during recovery from a fatiguing contraction," *J. Appl. Physiol.*, vol. 67, no. 2, pp. 648-654, 1989.

[39] J. Wan, Z. Qin, P. Wang, Y. Sun and X. Liu, "Muscle fatigue: general understanding and treatment," *Experimental & Molecular Medicine*, vol. 49, no. 10, pp. e384-e384, 2017.

[40] S. Lewis et al., "Fully Implantable Multi-Channel Measurement System for Acquisition of Muscle Activity," *IEEE Trans. Instrum. Meas.*, vol. 62, no. 7, pp. 1972-1981, 2013.